

# Reconstruction of the local density of states in Ag(111) surfaces using scanning tunneling potentiometry

J. Homoth, M. Wenderoth,\* K. J. Engel, T. Druga, S. Loth, and R. G. Ulbrich

*IV. Physikalisches Institut der Universität Göttingen, Friedrich-Hund-Platz 1, D-37077 Göttingen, Germany*

(Received 17 August 2007; revised manuscript received 1 October 2007; published 20 November 2007)

We present scanning tunneling microscopy data on clean Ag(111) surfaces in UHV. Standing-wave patterns of the surface state are investigated to study the influence of a thermal step across the tunnel junction on constant current topographies. When constant current topographies are measured at bias voltages below 10 mV with temperature differences of more than a few kelvins between tip and sample, the apparent corrugation is drastically increased. Constant current topographies at low bias voltages and finite temperature differences do not reveal the true local density of states of the surface. The apparent corrugation is caused by a spatially varying thermovoltage superimposed to the bias voltage while scanning the sample's local density of states. With the help of scanning tunneling potentiometry, the correct local density of states of the sample can be reconstructed.

DOI: 10.1103/PhysRevB.76.193407

PACS number(s): 73.50.Lw, 73.20.At, 07.79.Cz

## I. INTRODUCTION

Constant current topography (CCT) is one of the standard modes in which a scanning tunneling microscope (STM) is usually operated. The sample bias voltage  $V_{bias}$  is set to a constant value, and via a feedback loop, the tunneling current is kept constant while scanning the surface. Following the theory by Tersoff and Hamann, data obtained at sufficiently low  $V_{bias}$  are interpreted as surfaces of constant local density of states (LDOS)  $\rho(E, x, y)$ .<sup>1</sup> One fundamental assumption of this interpretation is that the applied  $V_{bias}$  is independent of the tip's position. If tip and the sample of an STM are at different temperatures, this assumption is no longer valid and a spatially varying thermovoltage  $V_{th}(x, y, z)$  must be considered.<sup>2</sup> The difference in temperature shapes different Fermi distributions for the occupancy of electronic states in the two electrodes. This causes a net current of thermally excited electrons. The thermovoltage results from the balance between forward and backward tunneling. Stövneng and Lipavský have shown that this voltage depends on the gradient  $\partial\rho(E, x, y)/\partial E$  of the LDOS with respect to the Fermi energy ( $E_f$ ),

$$V_{th} = \frac{\pi^2 k_B^2 (T_t^2 - T_s^2)}{6e} \left( \frac{1}{\rho_t} \frac{\partial \rho_t}{\partial E} + \frac{1}{\rho_s} \frac{\partial \rho_s}{\partial E} + \frac{z}{\hbar} \sqrt{\frac{2m_0}{\phi}} \right) \Bigg|_{E=E_f}, \quad (1)$$

where  $\rho_t$  and  $\rho_s$  denote the tip and sample densities of states, respectively,  $T_t$  and  $T_s$  their temperatures, and  $\phi$  the apparent barrier height.<sup>2</sup> This is an important extension of the common interpretation since a spatially varying  $\partial\rho_s(E, x, y)/\partial E|_{E=E_f}$  results in  $V_{th}(x, y, z)$  variance on the same length scale. It is justified to neglect thermovoltages if  $V_{bias}$  (typically above 10 mV) is large compared with  $V_{th}$  (typically 1–500  $\mu$ V at  $\Delta T \approx 1$ –10 K).

First experimental investigations of thermovoltages in STM were performed by Williams and Wickramasinghe on MoS<sub>2</sub> at ambient conditions.<sup>3</sup> They demonstrated the sensitivity of  $V_{th}$  to chemical-potential variations on an atomic scale. Hoffmann *et al.* studied the thermovoltage signal on noble metal surfaces.<sup>4–6</sup> The thermovoltage signal in the vi-

cinity of surface steps was described in detail based on the approach by Stövneng and Lipavský. Moreover, thermovoltages were used to measure the mean free path of surface state electrons on Au(111).<sup>7</sup>

These investigations focused on the thermovoltage signal itself and regarded the CCT data as unaffected by thermovoltages. In contrast, this Brief Report concentrates on the importance of thermovoltages on the interpretation of STM data. Our approach allows a simultaneous mapping of (i) the standard CCT, (ii) separated  $V_{th}(x, y, z)$ , and (iii) CCT with  $V_{th}(x, y, z)$  compensated. We present data where the topography is significantly affected by thermovoltages and thus different from the “true” electronic structure of the surface. We conclude that in the presence of tip-sample temperature differences, only CCT data with compensated  $V_{th}(x, y, z)$  represent the correct LDOS in the spirit of Tersoff and Hamann.

## II. EXPERIMENTAL SETUP

The experiments were performed in a Besocke-type STM system operating in UHV at a base pressure better than  $5 \times 10^{-11}$  mbar. We use a low temperature scanning tunneling potentiometry microscope that compensates  $V_{th}(x, y, z)$  at every scan point with an accuracy of 1  $\mu$ V by a second, interlaced feedback loop.<sup>7,8</sup> At first, the tip-sample distance is controlled in the usual constant current mode to measure the CCT. The tip  $z$  position is then subsequently fixed for up to 100 ms sampling intervals, and the tip-sample voltage is adjusted to zero net tunneling current.  $V_{th}(x, y, z)$  is denoted here as the tip-sample potential difference necessary for a zero compensation of the tunneling current.

The low temperature system allows *in situ* tip and sample exchange and optical access to heat the tip by light irradiation. The setup is mounted and shielded on the bottom of a liquid He tank. The liquid He shields themselves are shielded by liquid N<sub>2</sub> shields. Optical access is possible through small windows in the shields blocking infrared irradiation with thermally well-conducting quartz glasses (SUPRASIL®). Furthermore, the STM tip is thermally coupled to the He tank by a couple of silver wires. In this way, tip and sample

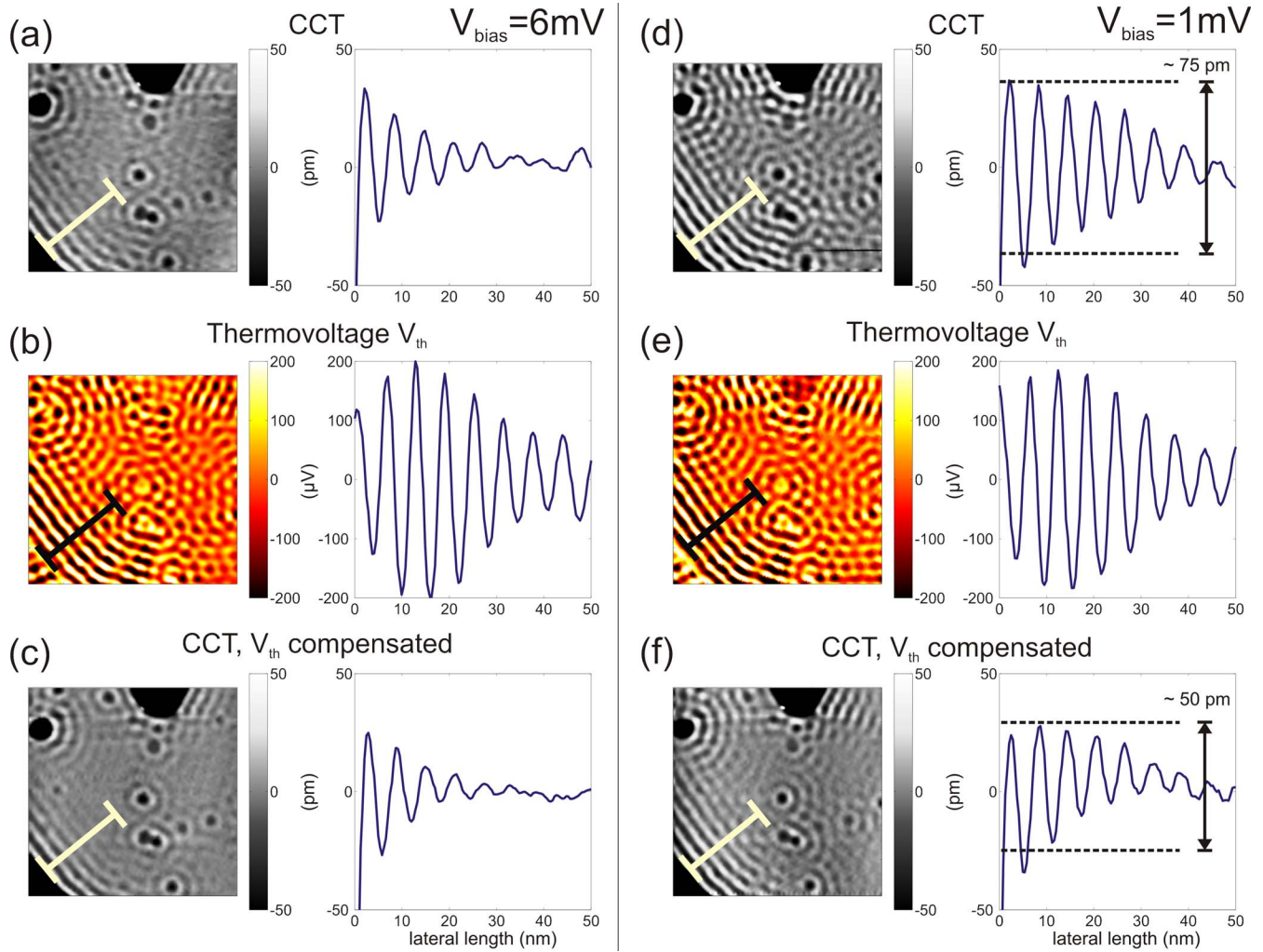


FIG. 1. (Color online) STM data on Ag(111) at  $T_t=33$  K and  $T_s=8$  K determined by the fit to theory as presented here. (a) Constant current topography acquired at a sample bias of 6 mV and the tunnel current set to 3 nA. (b) The acquired thermovoltage data alone and (c) constant current topography with compensated thermovoltage. (d)–(f) illustrate the same area on the surface but acquired at a sample bias of 1 mV. Note the apparent increase of corrugation depth in CCT at low  $V_{bias}$  [(a) and (d)] caused by the superposition of  $V_{th}(x, y, z)$ . The weak differences between (c) and (d) are attributed to the finite dispersion of the surface state’s LDOS and the increasing lifetime close by  $E_f$ .

temperatures differ by less than 3 K. The base temperature of the STM without illumination is 5.6 K, measured by a calibrated silicon diode at the sample attachment. STM tips were made from electrochemically etched tungsten wire. *In situ* tip preparation includes cleaning by annealing and sharpening by  $Ar^+$  sputtering.

Silver films were grown on carefully degassed mica substrates at 500 K using e-beam evaporators at a deposition rate of 15 ML/min. Such films consist of (111) textured grains with large atomically flat terraces of up to  $1 \mu m^2$  in size. On this surface, a parabolic band of surface states forms, which hosts a two-dimensional electron gas of nearly free electrons with an effective mass of  $m^* = 0.4m_e$ .<sup>9</sup> For the experiments reported here, Ag(111) was chosen for its simple structure with no surface reconstruction. Standing-wave patterns are observed in the vicinity of defects such as, e.g., adsorbates and island steps. These patterns are formed by coherent superposition of incident and reflected surface state waves. A temperature difference between tip and sample

was maintained by using a white light-emitting diode (LUXEON® K2 from Philips) as a cold-light source. The tip was heated by irradiation, and the positioning was examined with an optical microscope.

### III. RESULTS

Figures 1(a) and 1(d) show CCT data of the Ag(111) surface at different  $V_{bias}$ . An interference pattern of the surface state, which is scattered at a monatomic step on the surface, is evident. The onset of the surface state is measured 65 meV below  $E_f$  by  $dI/dV$  spectroscopy, which is consistent with earlier investigations.<sup>9</sup> The same area was imaged without [see Figs. 1(a) and 1(d)] and with [see Figs. 1(c) and 1(f)] compensation of the thermovoltage across the tunnel junction. The simultaneously acquired thermovoltage is plotted in Figs. 1(c) and 1(e). Cross sections through the data are presented next to the images. It is worth noting that the thermovoltage is phase shifted by nearly  $\pi/2$  in comparison with

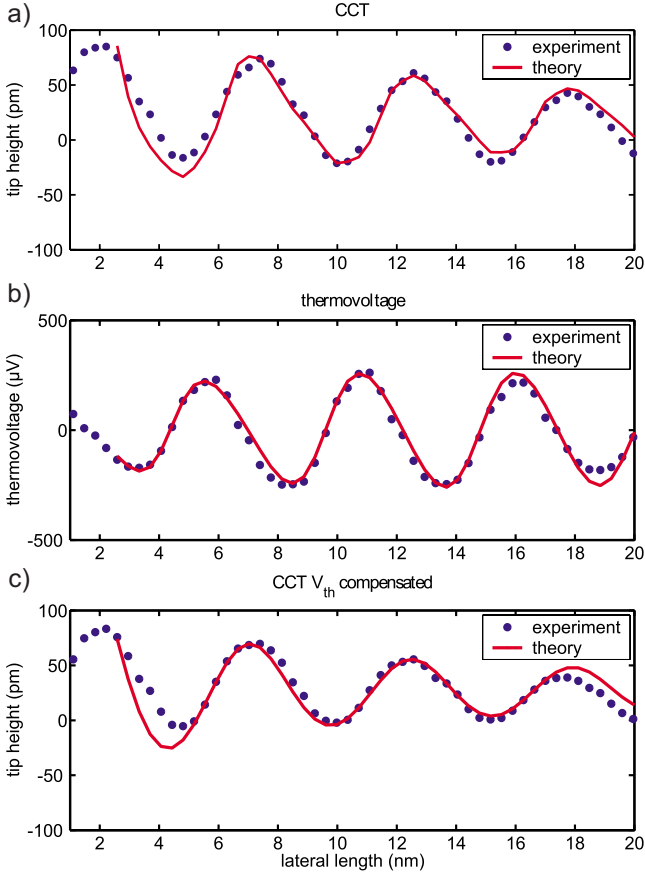


FIG. 2. (Color online) (a) Comparison of the analytically derived  $z(x)$  (solid red/gray) in the vicinity of a scattering step with measured CCT without compensated thermovoltage (blue/dark gray dots). (b) Comparison of the analytically (solid red/gray) and experimentally (blue/dark gray dots) derived thermovoltages. (c) depicts the height contour with compensated thermovoltage (blue/dark gray dots) in comparison with the analytically calculated  $z(x)$  (solid red/gray). From Eq. (6), the temperatures of tip and sample are derived to be 33 and 8 K, respectively. A transmission probability through the step of 70% is evaluated.

the CCT signal excluding thermovoltages. The apparent corrugation of CCT images without compensated thermovoltage is increased. The cross sections in Figs. 1(a) and 1(d) can thus be explained by the “true LDOS,” measured with a bias voltage which is superimposed by the spatial varying thermovoltage. A more quantitative comparison can be done by analyzing the standing-wave pattern at the steps. Tersoff and Hamann assumed a LDOS described by

$$\rho_s(\vec{r}, E) = e^{-\alpha z} \rho_s(x, y, E), \quad (2)$$

where  $\rho_s$  denotes the LDOS of the sample times the decay perpendicular to the surface. In the vicinity of a straight, infinite long step, the LDOS of the surface state  $\rho_{ss}(r, E)$  is modulated by the superposition of incident and reflecting waves,

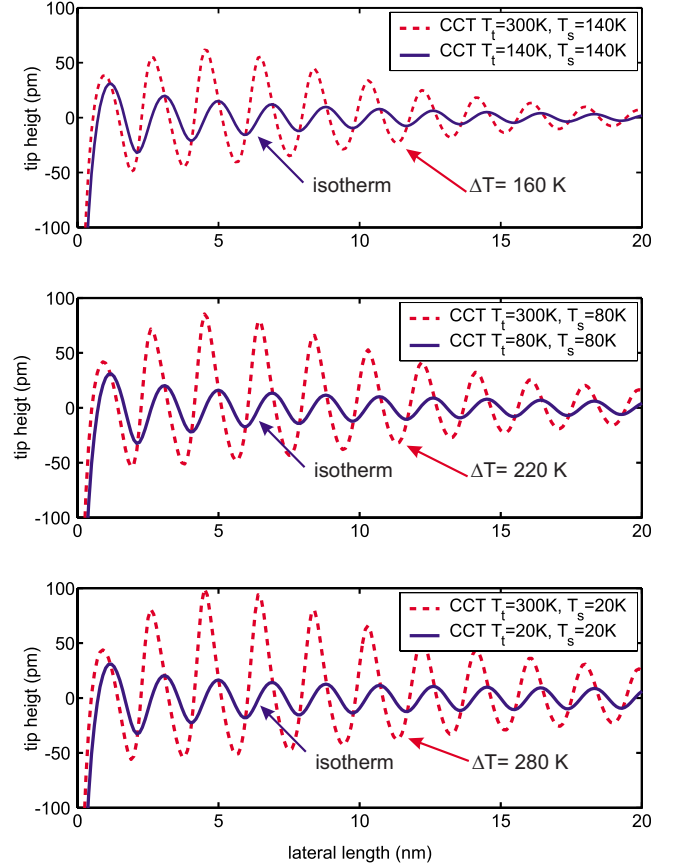


FIG. 3. (Color online) Analytically derived CCT of the surface state of Au(111) ( $E_f=410$  meV and  $m^*=0.25m_e$  taken from Ref. 11) in the vicinity of a scattering step ( $R=100\%$ ). Calculations were performed for  $V_{bias}=5$  mV. Solid blue/dark gray curves represent equal temperature of tip and sample, whereas the red/gray dashed curves represent typical situations of VT-STMs with tip and sample at different temperatures.

$$\rho_{ss}(\vec{r}, E) = \frac{m^*}{\pi\hbar} e^{-\alpha z} [1 - RJ_0(2kx)], \quad (3)$$

where  $J_0$  is the Bessel function of first kind and zero order.  $R$  describes the reflectivity of the step, and  $k$  depicts the  $k$  component of the wave vector perpendicular to the step at the energy  $eV_{bias}$ . We have derived an analytical expression for the height contour as well as the thermovoltage. Since their derivations are lengthy, we refer to Ref. 10 for further details. We note the following conditions to account for the applied approximations: (i)  $eV_{th} \ll k_B T_{t,s}$ , (ii)  $4k_B T_{t,s} \partial \rho_{ss} / \partial E \ll \rho_{ss}$ , and (iii)  $4k_B T_{t,s} \ll E_f$ . The tip height in the vicinity of an extended step in the  $y$  direction is derived as

$$z(x) = z_0 + \frac{1}{\alpha} \ln[1 - CJ_0(2kx)h_n(x)], \quad (4)$$

$$h_n(x) = \frac{1}{2} \left( \frac{S_t}{\sinh(S_t)} + \frac{S_s}{\sinh(S_s)} \right), \quad (5)$$

with  $S_t = \pi k_f x k_B T_t / E_f$  and  $S_s = \pi k_f x k_B T_s / E_f$ ,  $T_t$  and  $T_s$  denoting tip and sample temperatures, and  $C$  describing the part of

the tunneling current, which is carried by surface states in the absence of a reflecting step. Equation (4) describes the tip height with tip and sample at different temperatures but compensated  $V_{th}$ . CCT data including the cross-talk of thermovoltage, as measured in usual CCT, is described by

$$z(x) = z_0 + \frac{1}{\alpha} \ln \left( \frac{1 - CJ_0(2kx)h_N(x)}{1 - V_{th}(x,y,z)/V_{bias}} \right). \quad (6)$$

In the limit of  $V_{th} \ll V_{bias}$ , expression (4) is obtained. Equation (6) denotes that lower  $V_{bias}$  increases the effect of  $V_{th}$ . Therefore, the true LDOS is acquired at high  $V_{bias}$ , but local thermovoltages dominate the apparent corrugation when  $V_{th}$  is on the same order of magnitude. A comparison of theoretical derived thermovoltage and CCT data with experimental data is presented in Fig. 2. Figure 2(a) shows a section through the CCT data without compensated thermovoltage, while Fig. 2(b) presents the thermovoltage, itself. The compensated CCT signal is shown in Fig. 2(c). It is worth noting that all features, e.g., phase shift of  $\pi/2$ , amplitude, and decaying behavior, are very well reproduced. The tip and sample temperatures are evaluated to 33 and 8 K, respectively.

#### IV. DISCUSSION

Our results demonstrate that data taken in STMs with tip and sample at different temperatures have to be interpreted with care. Prominent and important examples are variable temperature STMs (VT-STMs). The tips of VT-STMs are typically at room temperature, while the sample is at tem-

peratures down to 20 K. Since the thermovoltage strength increases quadratically with temperature difference, strongly modified CCTs are expected at higher temperature differences. Figure 3 demonstrates the influence of temperature differences for the Au(111) surface state in the vicinity of a scattering step. This is a widely investigated system. With a finite temperature difference, the apparent corrugation (dashed red) first increases to a certain maximum and then decreases monotonically. Enhanced corrugation amplitudes caused by the cross-talk of thermovoltages are observed. This is in strong contrast to the isothermal case (solid blue), where the height contour decreases monotonically with no enhanced corrugation amplitudes.

#### V. CONCLUSION

The influence of a thermal gradient across a tunnel junction of an STM on CCT was investigated. In the  $V_{bias}$  range of some mV and with a temperature difference between tip and sample of only 25 K the corrugation is drastically increased. The CCT data do not show the true LDOS of the surface but a masked LDOS dominated by thermovoltages across the tunnel junction. By applying the technique of Scanning Tunneling Potentiometry the true LDOS information is recovered. Our finding may help to improve the quantitative interpretation of existing CCT data.

#### ACKNOWLEDGMENT

This work was supported by the Deutsche Forschungsgemeinschaft as part of SFB 602 Tp A7, A3 and the German National Academic Foundation.

\*wendero@physik4.gwdg.de

<sup>1</sup>J. Tersoff and D. R. Hamann, Phys. Rev. B **31**, 805 (1985).

<sup>2</sup>J. A. Stövneng and P. Lipavský, Phys. Rev. B **42**, 9214 (1990).

<sup>3</sup>C. C. Williams and H. K. Wickramasinghe, Nature (London) **344**, 317 (1990).

<sup>4</sup>D. Hoffmann, J. Y. Grand, R. Möller, A. Rettenberger, and K. Läger, Phys. Rev. B **52**, 13796 (1995).

<sup>5</sup>D. Hoffmann, A. Haas, T. Kunstmann, J. Seifritz, and R. Möller, J. Vac. Sci. Technol. A **15**, 1418 (1997).

<sup>6</sup>D. Hoffmann, J. Seifritz, B. Weyers, and R. Möller, J. Electron Spectrosc. Relat. Phenom. **109**, 117 (2000).

<sup>7</sup>K. J. Engel, M. Wenderoth, N. Quaas, T. C. G. Reusch, K. Sautthoff, and R. G. Ulbrich, Phys. Rev. B **63**, 165402 (2001).

<sup>8</sup>A. Schneider, M. Wenderoth, K. Engel, M. Rosentreter, A. Heinrich, and R. Ulbrich, Appl. Phys. A: Mater. Sci. Process. **66**, S161 (1998).

<sup>9</sup>O. Jeandupeux, L. Bürgi, A. Hirstein, H. Brune, and K. Kern, Phys. Rev. B **59**, 15926 (1999).

<sup>10</sup>K. J. Engel, Ph.D. thesis, Universität Göttingen, 2001, <http://webdoc.sub.gwdg.de/diss/2002/engel/index.html>

<sup>11</sup>S. D. Kevan and R. H. Gaylord, Phys. Rev. B **36**, 5809 (1987).